Chromosome architecture in the decondensing human sperm nucleus

Olga Mudrak[1,2], Nikolai Tomilin[2] and Andrei Zalensky[1,*]

[1]The Jones Institute for Reproductive Medicine, Eastern Virginia Medical School, Norfolk, VA 23507, USA
[2]Institute of Cytology, Russian Academy of Sciences, St Petersburg, 194064, Russia
*Author for correspondence (e-mail: zalensao@evms.edu)

Summary

Whereas recent studies demonstrated a well-defined nuclear architecture in human sperm nuclei, little is known about the mode of DNA compaction above the elementary structural unit of nucleoprotamine toroids. Here, using fluorescence in-situ hybridization (FISH) with arm-specific DNA probes of chromosomes 1, 2 and 5, we visualized arm domains and established hierarchical levels of sperm chromatin structures. The compact chromosome territories, which in sperm have a preferred intranuclear localization, have an extended conformation represented by a 2000 nm chromatin fiber. This fiber is composed of a 1000 nm chromatin thread bent at 180° near centromere. Two threads of 1000 nm, representing p-arm and q-arm chromatin, run in antiparallel fashion and join at the telomeres. Each 1000 nm thread, in turn, resolves into two rows of chromatin globules 500 nm in diameter interconnected with thinner chromatin strands. We propose a unified comprehensive model of chromosomal and nuclear architecture in human sperm that, as we suggest, is important for successful fertilization and early development.

Key words: Sperm, Nucleus, Chromosome, In-situ hybridization, Fertilization

Introduction

During the last quarter of the past century, evidence has accumulated that, in interphase cells, an ordered and dynamic global architecture of chromosomes exists and is involved in a variety of nuclear functions (for reviews, see van Driel et al., 2003; Taddei et al., 2004; Cremer et al., 2004). The central concept of this hypothesis, the chromosome territorial organization (Stack et al., 1977; Schardin et al., 1985), has been proved (Cremer and Cremer 2001; Cremer et al., 2004). Current studies concentrated on the elucidation of higher order chromatin structures and chromosome path within the chromosome territory (CT) (Belmont et al., 1999; Stadler et al., 2004; Lowenstein et al., 2004) and also the relative spatial arrangement of individual CTs (Parada et al., 2004).

Cremer and co-authors proposed that "the nuclear architecture – in addition to DNA sequence level and histone code – is an integrated part of the epigenetic mechanisms" (Cremer et al., 2004). In this context, specific and well-organized nuclear organization recently demonstrated for human sperm cells may be of special interest. It has been shown in these cells that, (1) Individual chromosomes occupy distinct territories (Haaf and Ward, 1995; Zalensky et al., 1995); (2) each chromosome has a defined intranuclear localization and the relative positioning of chromosomes is non-random (Geraedts and Pearson, 1975; Luetjens et al., 1999; Hazzouri et al., 2000; Tilgen et al., 2001; Zalenskaya and Zalensky, 2004); (3) centromeres (CENs) are collected into a compact chromocenter that is buried within a nuclear volume (Zalensky et al., 1993; Zalensky et al., 1995; Haaf and Ward, 1995; Hoyer-Fender et al., 2000); (4) telomeres (TELs) are localized at the nuclear periphery where they interact in dimers and tetramers (Zalensky et al., 1995; Zalensky et al., 1997; Meyer-Ficca et al., 1998; Hazzouri et al., 2000); and (5) TEL dimers result from specific interactions between the two tips of each chromosome and, therefore, chromosomes in sperm are looped (Solov'eva et al., 2004).

Within this model of genome architecture in human sperm, structural organization of chromosomes remain largely unresolved. Since it had been established that basic chromosomal proteins in mammalian sperm (protamines) were drastically different from proteins of somatic cells (histones), numerous efforts were directed to understand the fundamental structure formed when genomic DNA is packaged by protamines (Luzatti and Nikolaieff, 1959; Sobhon et al., 1982; Balhorn, 1982; Fita et al., 1983). Studies of the nucleoprotamine structure resulted in authenticating the elementary unit of DNA packaging into toroids both in vitro (Allen et al., 1997; Brewer et al., 1999; Brewer et al., 2003) an in vivo (Hud et al., 1993; Balhorn et al., 1999). On the higher structural level, it has been proposed that chromatin in mammalian sperm is organized into loop domains attached at their bases to a nuclear matrix (Ward and Coffey, 1991; Yaron et al., 1998; Ward and Ward, 2004). Looped organization of sperm DNA is disputed in other works (Sanchez-Vazquez et al., 1998).

This study partially fills the noticeable gaps between our knowledge of the elementary DNA-protamine structure and the higher-order chromosome packing in human sperm cells. Using epifluorescence microscopy following two-color fluorescence in-situ hybridization (FISH) with micro-dissected

probes for the p-arms and q-arms of the large metacentric chromosome 1 and chromosome 2 (CHR1 and CHR2), and the large submetacentric chromosome 5 (CHR5), we dissected the internal organization of CTs, and describe here successive hierarchies of chromosome structures. Based on acquired data and data that had already been published, we propose a consensus model of DNA compacting in sperm, starting with the protamine toroids as an elementary unit followed by the well-defined higher-order chromosome architecture.

Materials and Methods

Cell preparation for in-situ hybridization

Human sperm cells were obtained from the semen of 10 healthy, fertile donors. Sperm concentrations and motilities were determined by computer-assisted semen analysis; mean sperm concentration $25 \pm 2 \times 10^6$ sperm/ml, motility $52 \pm 2\%$. Sperm cells in all samples had normal morphology (>30% normal forms, WHO criteria). The study was approved by the IRB at UC Davis School of Medicine and Eastern Virginia Medical School.

During preliminary studies, we did not observe noticeable differences between samples obtained either from different donors or between sperm in the motile fraction acquired by swim-up and total semen. Therefore, the majority of experiments had been performed using total semen.

Sperm cells were washed with PBS, resuspended in 30% glycerol-PBS and stored in aliquots at –80°C. Essentially, cells were prepared for FISH as described earlier (Zalensky et al., 1995; Zalensky et al., 1997; Zalenskaya and Zalensky, 2004). Briefly, cells were fixed with 0.5% formaldehyde-PBS and decondensed in 10 mM DTT, 0 to 0.5 mg/ml heparin in PBS for 30 minutes at room temperature. Treatment with DTT-heparin induces uniform nuclear swelling, while preserving nuclear shape; the higher the heparin concentration, the higher the resulting nuclear decondensation (Delgado et al., 1980; Zalensky et al., 1993). Such swelling is a prerequisite to perform FISH in human sperm cells (Zalensky et al., 1993; Zalensky et al., 1995). Decondensed cells were loaded onto microscope slides, air-dried, washed in 2×SSC, water, dehydrated in a 70% to 100% ethanol series and air-dried again.

DNA probes for FISH, and antibodies

Digoxigenin (DIG-) and biotin (BIO-) labeled arm-specific chromosome probes BIO-1p, DIG-1q, BIO-2p, DIG-2q, DIG-5p, BIO-5q and sub-TEL-specific probes were from A.L. Tech. Biomedical Inc. FITC-labeled sheep anti-DIG, FITC-labeled rabbit anti-sheep, and FITC-labeled goat anti-rabbit antibodies were from Roche; Texas Red (TR) labeled avidin (AV) and biotinylated anti-AV were from Vector Inc.

FISH and microscopy

Sperm cells were denatured in 70% formamide, 2×SSC at 72°C for 3 minutes. Nuclear DNA was fixed in the denatured state by immediate immersion of the slide into cold 100% ethanol. Hybridization and post-hybridization washings were performed according to manufacturer's instructions. In a typical experiment, a mixture of equal volumes DIG-labeled q-arm and BIO-labeled p-arm probes were denatured, re-annealed for 10 minutes at 37°C, and applied to a slide. Overnight hybridization at 37°C was followed by a wash in 50% formamide in 2×SSC at 45°C. Slides were blocked in 3% bovine serum albumin (BSA), 0.2% Tween-20 in 4×SSC for 30 minutes at room temperature and subjected to detection and amplification steps as follows. First, slides were incubated with sheep anti-DIG-FITC antibodies (1:100) and AV-TR (1:200), then with rabbit anti-Sheep-FITC antibodies (1:200), and BIO-anti-AV (1:100), and finally with goat anti-rabbit-FITC antibodies (1:200) and AV-TR (1:100). Each step was carried out for 30 minutes at 37°C. Between amplification steps, slides were washed three times for 5 minutes in 0.2% Tween-20 in 4×SSC at 45°C and blocked for 5 minutes.

Slides were mounted using Vectashield medium (Vector). Hybridization results were visualized using a Leitz Ortholux microscope and an oil immersion 60× with a 1.4 NA objective. Images were collected using a MagnaFire digital color camera and MicroFire software (Optronics Inc.). For each nuclei, four images were taken with selective filters (Texas Red only, FITC only, DAPI only and multi-band-pass filter). At least 200 images for each combination of hybridization probes were collected. Images were processed with Adobe Photoshop 7.0 software. Intranuclear positioning of the compact CTs relative to the tail-attachment point were determined as described earlier (Zalenskaya and Zalensky, 2004). Distances were measured using Sigma Scan Pro 5.0 software. Typically, about 100 nuclei demonstrating similar structural elements (e.g. chromatin fibers, globules, etc.) were analyzed. Statistical analysis was performed in Microsoft Excel with added Analyze-It software.

Results

Compact CTs

In human sperm cells, protamines electrostatically neutralize and pack DNA into condensed chromatin, the intermolecular net of disulfide bridges between protamines providing additional compactness (Balhorn, 1982). Reduction of disulfide bonds with DTT or similar agents results in the slight swelling of sperm nuclei that is crucial for penetration of DNA probes and antibodies during FISH. Polyanionic polysaccharide heparin weakens DNA-protamine interactions and partially relaxes the chromatin structure (Villeponteau, 1992). Treatment of sperm cells with DTT-heparin results in uniform swelling of sperm nuclei (Zalensky et al., 1993) and has been used throughout this work.

Fig. 1A-C provides representative patterns of two-color FISH with p-arm- and q-arm-painting probes in minimally decondensed sperm cells. In the vast majority of sperm nuclei, FISH signals originating from two arms overlapped or were closely located together, and were therefore restricted to a compact CT. Size measurements demonstrated that the area of sperm CT is about four times less than the area of metaphase chromosomes; therefore, CT in sperm is much more condensed.

Images that were registered using selective filters show that signals produced by p- and q-arms are similar in shape and size (Fig. 1A-C), which may correspond to the parallel stacking or intermingling of the arms. However, further details of chromosome-arm structural organization, e.g. their trajectories or particulars of relative spatial localization, cannot be resolved at this degree of nuclei swelling.

Systematic observations of intranuclear localization of the CT relative to the tail-attachment point as described in details by Zalenskaya and Zalensky (Zalenskaya and Zalensky, 2004), demonstrated preferential positioning for each of the three chromosomes studied, Fig. 1D. In 90% of cells, CHR1 was found in the apical half of the nucleus, whereas the distribution along the short axes of nuclear ellipsoid was random. Both CHR2 and CHR5 were preferentially (80% and 85%, respectively) located in the basal half of the sperm nucleus.

Internal structural organization of the CT

To explore details of higher-order chromosome organization, sperm cells were decondensed with 0.5 mg/ml heparin, 10 mM DTT. Owing to this treatment, the nuclear size – as determined by the long axis length – increased approximately 1.5 to 2 times in the majority of cells, resulting in the enlargement of compact CTs and the visibility of trajectories of chromosome arms. In all experiments, care was taken to maintain the 3D-structure of the nuclei as much as possible. For this reason, mild formaldehyde fixation was used before treatment with heparin-DTT.

Upon examination of at least 200 images of each chromosome, we noticed several repetitive structural patterns of chromatin fiber conformations. Assessment was performed on nuclei with uninterrupted and traceable FISH signals that originated from both arms, in which localization of the TEL and CEN regions could be unequivocally assigned. Fig. 2A provides an example of CEN and TEL identification. In >90% of cells, the hybridization from both arms overlaps near the CEN, resulting in a bright yellow signal in merged images and/or images taken with a triple-band-pass filter (Fig. 2A, two right columns). Localization of the arm tips (of TELs) in some experiments was ascertained using simultaneous hybridization with arm-specific subtelomeric probe (Fig. 2A). Notice that, in most cases such hybridization was not necessary because TELs were easily located as the regions at extreme distance along trajectories of the arms from the yellowish CEN region.

Fig. 2B-D illustrates the relative arrangement of the p- and q-arms in large metacentric (CHR1 and CHR2) and submetacentric (CHR5) chromosomes. The CT is not composed of randomly packed chromatin fibers but rather, each chromosome arm manifests individuality. In the majority of cells, all chromosomes demonstrated overall extended conformation with the CT stretched along the long nuclear axis. Near-CEN chromosome fibers bend almost at 180° so that p- and q-arms are aligned in the antiparallel fashion. Such antiparallel packing of the arms produces a hairpin structure of chromosomes with the two TELs close to each other or superimposed (Fig. 2Ba-d, Ca,b, Da,b). Chromatin fibers of p- and q-arms are also braided around each other, at least within some regions of the CTs (Fig. 2Ba,b,d, C,a).

In nuclei swollen to a higher degree, hairpin CTs often untwisted to almost linear structures, resembling metaphase chromosomes (Fig. 2Be, Cd,e, D,c). At this stage of decondensation, p-arm and q-arm domains were spatially separated, and this separation was particularly pronounced in CHR5 (Fig. 2Cd,e). The average length of the extended untwisted CHR1 territory in sperm was 10.2±0.3 μm, with an average diameter of 2±0.2 μm. For comparison, the average dimensions of the same chromosome in metaphase was 5.7×2 μm.
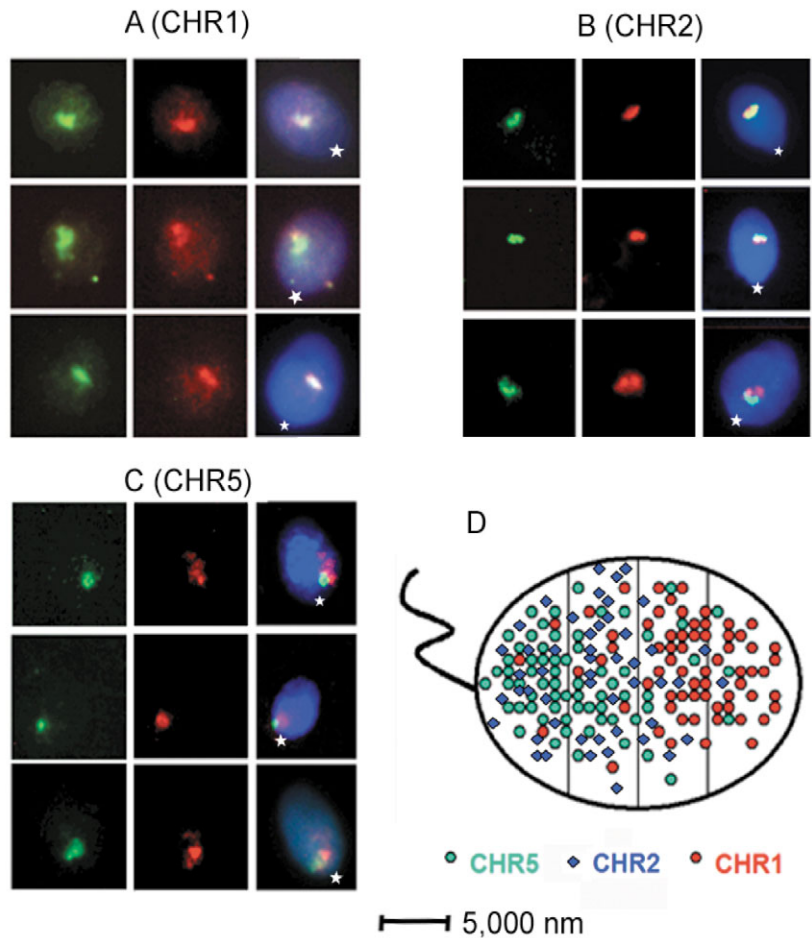

Fig. 1. Compact CTs in human sperm nuclei. (A-C) Localization of chromosome arms using FISH with arm-specific microdissected DNA probes. Left panels, DIG-labeled q-arm probes detected with anti-DIG-FITC; middle panels, BIO-labeled p-arm probes detected with avidin-TR; right panels, images of the same cells registered using triple-band-pass filter, total DNA counterstained with DAPI. Position of the tail attachment (basal part of nuclei) is indicated by a star. (D) Non-random intranuclear localization of the compact CT of sperm chromosomes. Cumulative scheme, showing positions of CTs registered by FISH. Sperm cell nuclei is approximated by an ellipse and is divided into four zones, starting from the basal side that is determined by tail attachment site.

TEL and CEN domains

Fig. 3A,B illustrates progressive unfolding of the q-arm of CHR1 with increasing nuclear decondensation induced by heparin-DTT. At the initial stages, most cells demonstrated the club-like structure (Fig. 3A, upper left). At higher swelling, chromatin in the internal part of q-arm dispersed, while terminal domains resided in compact configuration (shown by arrowheads in Fig. 3B). These more compact parts of chromosome arms corresponded to heterochromatic regions close to the CEN and TEL. Localization of the region adjacent to CEN was established from two color FISH experiments, using probes for both arms of CHR1, as in Fig. 2B. The near-CEN region remained in the condensed state even in the highly swollen nuclei (shown by lines in Fig. 3A,B).

Arm-specific probes used in this work were obtained by microdissection. These probes did not hybridize to the CEN constriction and FISH signals did not overlap in metaphase
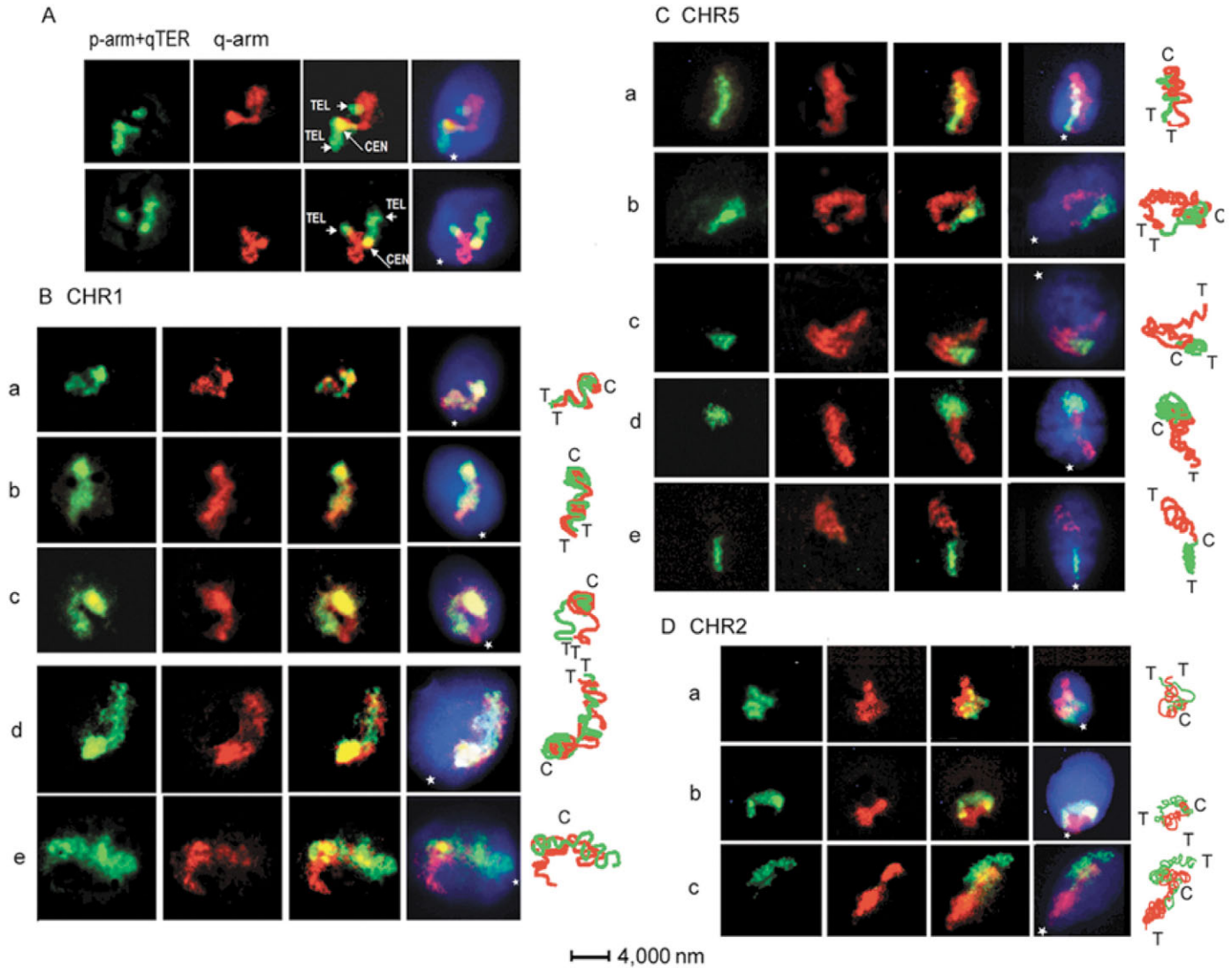
Fig. 2. Internal organization of CTs. (A) Identification of the TEL and CEN domains in CHR5 using simultaneous hybridization with arm-specific and subTEL-specific probes. Both rows of panels from left to right: DIG-labeled p-arm painting and q-arm subTEL probes (qTER) were detected with anti-DIG-FITC; BIO-labeled q-arm probe was detected with avidin-TR; merged image and image registered with triple-band-pass filter, total DNA counterstained with DAPI. (B-D) Localization of chromosome-arm domains with two-color FISH (p-arms, green; q-arms, red). Representative sperm cells are shown in the three rows of panels (from left to right): images taken with a selective green-filter; images taken with a selective red-filter; merged red and green images; images acquired using triple-band-pass filter. To the right of images: matching schemes of the chromosome-arm paths indicating the localization of TEL (T) and CEN (C). Position of the tail attachment (basal part of nuclei) is indicated by a star.

chromosomes (data not shown). Therefore, a prominent yellow FISH signal in sperm cells indicates highly condensed structure of the region adjacent to the CEN with intermingled p- and q-arm chromatin (Fig. 2).

The distance between TEL and CEN of the q-arm of CHR1 is strictly proportional to the length of the long axis of the nuclear ellipsoid (L) when L increases approximately 2.5 times, up to 16 µm (Fig. 3C). This linear relationship is highly significant (*P*<0.0001), and may reflect attachment of these heterochromatic regions to defined nuclear structures. Interestingly, the width of arm chromatin fiber did not change in the same interval of the long nuclear axis increase (Fig. 3D). The mean width of the chromosome arm fiber is 1000±120 nm. Furthermore, a frequency distribution plot (Fig. 3E) indicates

that this thickness is characteristic to the majority of cells. Relative constancy in this parameter reflects internal structural organization of the 1000 nm fiber as shown below. The structural parameters described here for the q-arm of CHR1, are inherent for small and long arms of all three chromosomes studied.

Internal structural elements of the chromosome arm fiber

In highly decondensed cells (L>17 µm), the length of the q-arm of CHR1 extends up to four times compared with the compact CT (Fig. 3B), in these cells the CHR1 q-arm is twice as long as in metaphase. At this state of swelling,
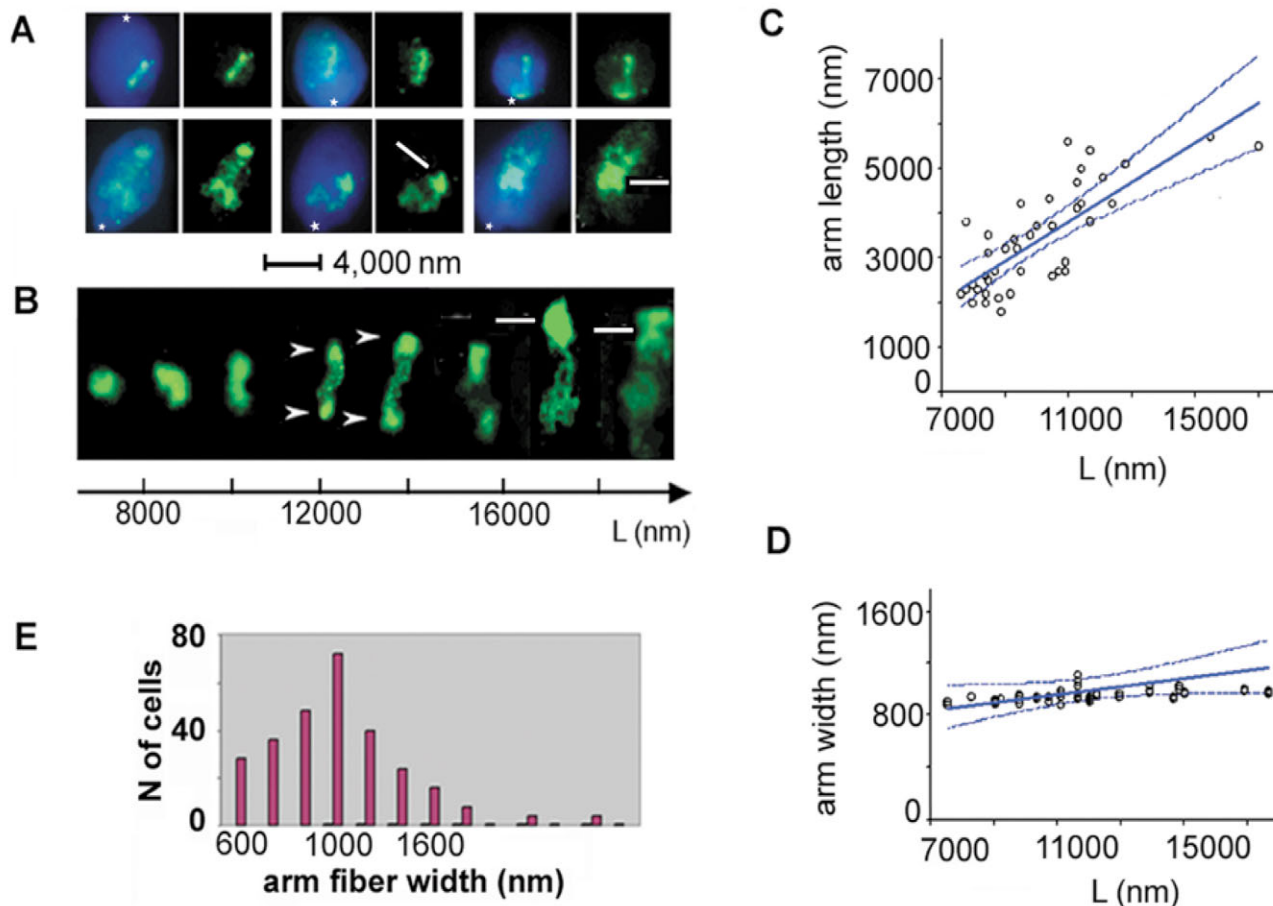
Fig. 3. Unfolding of the q-arm of chromosome 1. (A) Representative images of the CHR1 q-arm in sperm cells taken with triple-band-pass filter (DNA counterstained with DAPI, blue) or selective FITC-filter (green). (B) Selection of typical images of the CHR1 q-arm domain arranged in the order of nuclei size. L-length of the long nuclear axis. Position of the tail attachment (basal part of nuclei) is indicated by a star. Arrowheads in A and B show condensed heterochromatic regions and white lines the CEN domain. (C) Correlation between the lengths of CHR1 q-arm and the long nuclear axis in sperm cells. (D) The width of the CHR1 q-arm chromatin fibril does not depend on length of the long nuclear axis. D and C, solid bold lines show best-fit regression, dotted lines-confidence intervals. (E) Frequency distribution of the CHR1 q-arm widths registered over the wide interval of sperm nuclear sizes (0.4 μm>L<2.6 μm).

the 1000 nm fiber further unwinds and several recurring elements of the internal organization become visible (Fig. 4). First, each 1000 nm fiber appears to be composed of two chromatin strands (Fig. 4B, arrowheads). The limited resolution of conventional epifluorescence microscopy (~300 nm) does not allow to determine the relative strand localization (parallel or intertwined). Second, relatively dense globular beads interconnected by thinner and less dense chromatin filaments organize each strand (Fig. 4B, arrows). Diameters of these beads varied from 420nm to 550 nm, with a mean diameter of 480±60 nm. Importantly, the diameters of the two beads added together results in the observed thickness of the chromosome-arm fiber (1000 nm).

Discussion

In this work, we present evidence of archetypal modes of sperm-chromosome folding and packing, which was determined by observing the unwinding of the CT. We will discuss established elements of sperm-chromosome

organization in descending order of size, starting from the compact CT in 'native' nuclei.

Compact CTs and intranuclear positioning of chromosomes

In minimally swollen sperm cells, using two-color FISH with combinations of the arm-specific painting probes for CHR1, 2, and 5 we visualized tight CT formed by closely located *p*-and *q*-arms (Fig. 1). Territorial organization of human sperm chromosomes was observed earlier (Brandriff and Gordon, 1992; Zalensky et al., 1995; Haaf and Ward, 1995). According to our data, CT in sperm is approximately four times more condensed than in metaphase chromosomes, as evidenced by differences in lengths and widths of FISH signals. This roughly corresponds to the projected sixfold differences in DNA compaction (Balhorn, 1982; Ward and Coffey, 1991).

Compact CT in human sperm showed preferred intranuclear positioning (Fig. 1D). In 90% of cells, CHR1 was found in the apical half of the nucleus. 80% of CHR2 and 85% of CHR5 were preferentially located in the basal half.
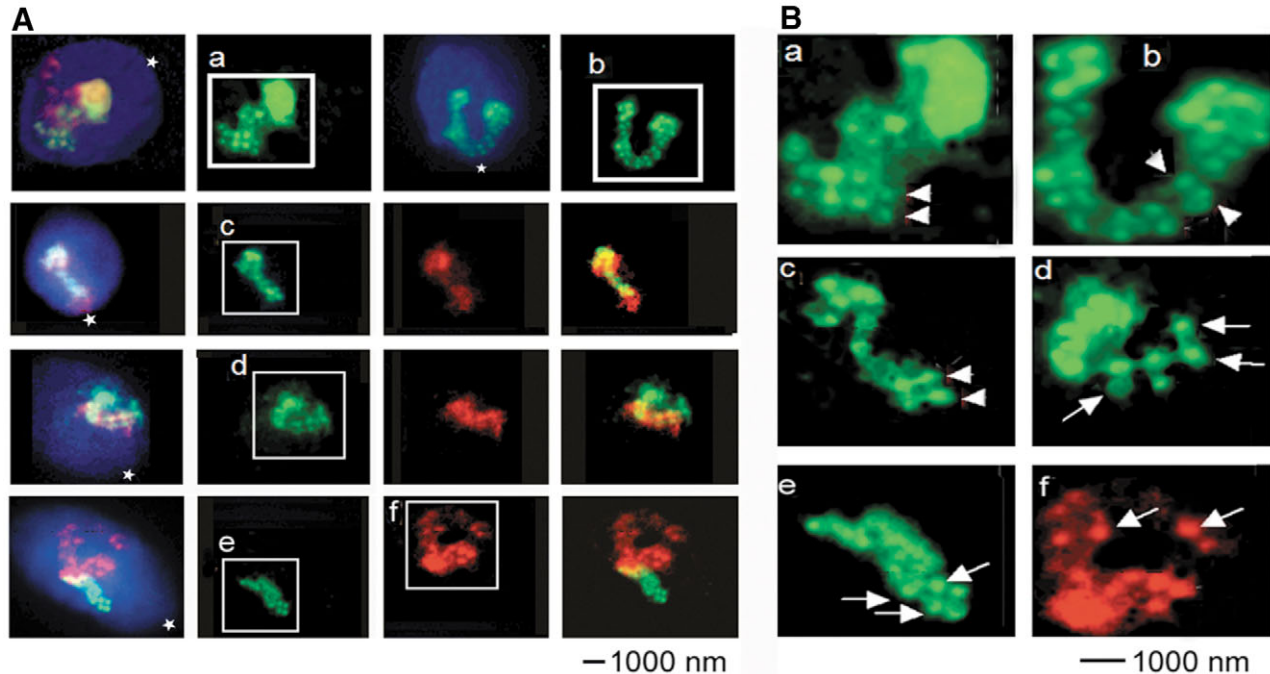
Fig. 4. Internal organization of chromosome arm fiber. (A) Representative images of CHR1 in cells with decondensed CTs. Representative sperm cells are shown in the four rows of panels. CHR1 q-arm, green; CHR1 q-arm, red. (First row) First and third images were taken with triple-band-pass filter; second and fourth with green-filter. (Third to fourth row, columns from left to right) Images taken with triple-band-pass filter; selective green-filter; selective red-filter; merged red and green images. (B) Enlarged images of the boxed areas. Globular chromatin nodules of approximately 500 nm are indicated by arrows. Arrowheads point at the double rows of globules that form fibers of chromosome arm chromatin.

Chromosome positioning in human sperm was studied earlier by using FISH with chromosome-painting probes (Luetjens et al., 1999; Hazzouri et al., 2000) and chromosome-specific centromeric probes (Zalenskaya and Zalensky, 2004). These works demonstrated sub-acrosomal localization of CHRX (Luetjens et al., 1999; Hazzouri et al., 2000; Zalenskaya and Zalensky, 2004), CHR1, and CHR6 (Zalenskaya and Zalensky, 2004), while CHR18 was found in the basal half (Luetjens et al., 1999). Noteworthy, sex chromosome X was found in a position close to the place of the first contact between sperm and egg cytoplasm, not only in humans but also in distant marsupial and monotreme mammals (Greaves et al., 2003), indicating the functional significance of such localization.

In somatic cells, the subnuclear confinement of a gene contributes directly to its expression (reviewed in Cockell and Gasser, 1999; Dundr and Misteli, 2001; Dietzel et al., 2004). Specific chromosome localization in sperm may determine an ordered activation of the paternal genome following fertilization (Schultz and Worrad, 1995; McLay and Clarke, 2003) and, therefore, might be important for successful fertilization and early development. It was proposed that, increased fertilization abnormalities and failures after introcytoplasmic sperm injection is associated with improper decondensation of chromosomes that are located in the apical part of the sperm nucleus (Terada et al., 2000).

In a range of somatic cells, the localization of CTs in the nuclear volume is closely related to their gene densities. Gene-dense chromosomes are located closer to the nuclei center (Boyle et al., 2001; Cremer et al., 2003). Recent experiments

(Gerlich et al., 2003; Walter et al., 2003) and computer simulations (Kreth et al., 2004) suggest the possibility of a global chromosome-positioning code that is maintained through the cell cycle. An ordered, relative position of chromosomes remains controversial. Some studies observed fixed chromosome positioning in the prometaphase-metaphase ring (Leitch et al., 1994; Nagele et al., 1995), whereas another study did not establish such order (Allison and Nestor, 1999). In any case, it would be interesting to compare the relative positioning of chromosomes in sperm, prometaphase plate and pronuclei to explore the possibility of the ordered positioning inheritance.

Hierarchical structural organization of chromosomes in sperm

When human sperm nuclei were pretreated with increasing physiological concentrations of heparin, condensed CT unraveled and chromosome arms developed into visible individual domains with traceable intranuclear paths (Fig. 2B-D). This allows sequential exposure of the structural elements of sperm chromosome organization by monitoring relative localization of chromosome arms within the CT. Using a similar approach, Dietzel and co-authors visualized distinct chromosome arms within CTs in human lymphocyte and amniotic fluid cell nuclei (Dietzel et al., 1998).

The procedure of sperm nuclear swelling using heparin and DTT mimics decondensation after fertilization, because both chemicals are analogs of components present in oocyte cytoplasm: disulfide-reducing glutathione (Sutovsky and

Schatten, 1997) and heparan sulphate (Romanato et al., 2003). Care was taken to maintain the 3D structure of the nuclei using DNA-protein crosslinking by mild formaldehyde fixation. Similar procedure was shown to be sufficient to reasonably maintain the size and shape of interphase nuclei (Dietzel et al., 1998).

At the initial stages of decondensation and in the majority of cells, CHRs1, 2 and 5 adopted extended territories that were oriented almost parallel to the long nuclear axis (Fig. 2B-D). Elongated shapes of chromosome in mouse and human sperm were observed using FISH with chromosome-specific DNA libraries (Haaf and Ward, 1985). Using chromosome-painting probes Hazzouri and co-authors showed the elongated shape of CHR13 and globular shape of CHR13 (Hazzouri et al., 2000). Strict comparison of data obtained in different laboratories is difficult because of different decondensation protocols and types of hybridization probes used.

In all three chromosomes studied, p- and q-arms were tightly blended together forming either aligned or intertwisted and spirally coiled structures (upper rows in Fig. 2B-D), the average width of the CT at this stage of nuclei swelling is around 2000 nm. Trajectories of arms in all chromosomes demonstrated a sharp (close to 180°) bend in the CEN vicinity, whereas the tips of p- and q-arms are located close to each other (Fig. 2B-D). Such structure corresponds to the earlier hypothesized hairpin conformation of chromosomes in human sperm (Zalensky et al., 1995) and is supported by specific dimeric interactions of TELs belonging to the p- and q-arms of each chromosome (Zalensky et al., 1997; Solov'eva et al., 2004).

When the size of the CT further increases, which corresponds to a higher nuclear swelling, chromatin fibers of arms partially separate (Fig. 2Bc, Cb,c, Db). In many nuclei, p- and q-domains develop into individual chromatin threads (Fig. 2B-D). These threads are characteristic of all chromosomes studied and had a mean width of around 1000 nm (Fig. 3D,E). Threads of 1000 nm often demonstrate spiral coiling; this was most clearly visualized in CHR5 (Fig. 2C-e). In some nuclei, chromatin fibers of both arms become spatially separated (Fig. 2Be, Cd,e, Dc). Such displacement would require unwinding and/or separation of the p- and q-domains intertwisted in the more compact CT.

We were able to observe the internal organization of 1000 nm chromatin threads in cells with partially relaxed CTs (Fig. 4). It appears that each 1000 nm thread is composed of two fibers (Fig. 4B, arrowheads), which in turn consists of the 500 nm chromatin beads (Fig. 4B, arrows) interconnected by thinner chromatin filaments. Theses beads were the smallest packaging unit of the sperm chromosome, we were able to register using the microscopy technique applied. Haaf and Ward, using FISH on sperm chromatin spreads, observed basic packaging units of 180±20 nm along with larger superbeads 360±30 nm and 600±60 nm (Haaf and Ward, 1995). In this work, harsh preparation of the extended chromatin fibers from sperm was used (2 M NaCl, 1% Triton X-100, ethanol), which might have induced protamine dissociation and redistribution. The chromatin beads of 500 nm observed by us might correspond to the 600 nm units, although it is difficult to compare data because of fundamentally different approaches of sample preparation. Combinations of nodular (beaded) and fiber (cord-like) structures in sperm chromatin were reported earlier: 'knobby' fibers 33-42 nm and 65-120 nm width laced together

by fine 6-8 nm strands (Sobhon et al., 1982); 'knobby' fibers 11 nm width (Fraschini and Biggiogera, 1985); 'hub-like' nuclear bodies with diameter of 10-100 nm, joined by a network of chromatin fibers (Sanchez-Vazquez et al., 1998); globular structures of 120-150 Å in diameter (Gusse and Chevaillier, 1980). These EM studies, while providing more accurate distance measurements, did not distinguish between chromatin belonging to different chromosomes and chromosome arms, whereas our approach, based on light microscopy, cannot provide structural data at distances less then 300 nm. In addition, methods of chromatin/nuclei preparation are drastically different. Therefore, structural parameters of sperm chromatin organization obtained in this work cannot be directly compared with the existing EM data. Chromosomes in sperm and interphase nuclei both have territorial organization, whereas sperm CTs are more compact and more structurally organized. Sperm CT organization appears to be uniform for different chromosomes whereas interphase CTs are highly dynamic and diverse. The latter is a logical reflection of their involvement in transcription, splicing and other cellular events (Dietzel et al., 2004; Cremer et al., 2004).

Compact heterochromatin regions near CEN and TEL

We demonstrated that, in the process of nuclear decondensation heterochromatic regions neighboring the TEL and CEN behaved differently from the rest of chromosome, and maintained compact conformation (Fig. 3A,B). The most stable was the near-CEN domain. Such enhanced stability of selected chromosomal domains towards the action of DTT/heparin may be associated with either specific primary structure of DNA and/or with specific nuclear proteins located in the CEN and TEL. Indeed, adenine stretches characteristic of centromeric DNA-repeats are considered important in controlling DNA curvature and the degree of centromeric chromatin compactness (Canapa et al., 2002). A good candidate protein is the heterochromatin protein 1 (HP1), a conserved chromosomal protein that is predominantly associated with the heterochromatin (reviewed by Eissenberg and Elgin, 2000). HP1 preferentially binds to condensed higher-order chromatin structures, and alters the chromatin-folding pathway to locally compact individual chromatin fibers without crosslinking them (Fan et al., 2004). In spermatids, HP1 is localized in a chromocenter (Martianov et al., 2002) a condensed structure formed by the association of CEN domains. HP1 is also associated with TELs in *Drosophila*, (Perrini et al., 2004). It would be of interest to establish the presence and nuclear localization of HP1 in human sperm.

During progressive nuclear swelling that leads to CT unpacking, the distance between the CEN and the TEL of a given chromosome arm is strictly proportional to the length of the long nuclear axis (Fig. 3C). Thus, linear stretching of a chromosome is proportional to nuclear stretching. This may be the result of physical links between TEL/CEN and defined cellular structures such as the nuclear membrane or nuclear matrix. Based on their localization, interactions between TELs and sperm nuclear membrane have been suggested (Haaf and Ward, 1995; Zalensky et al., 1997), and characteristics of the sperm TEL-binding complex (Gineitis et al., 2000). Although the chromocenter in human sperm has a defined intranuclear

position (Zalenskaya and Zalensky, 2004), its association with the nuclear matrix has not been demonstrated.

Models of the chromatin and chromosome architecture in human sperm

A model of defined and organized nuclear architecture in human sperm nuclei was proposed based on FISH data obtained with pan-centromeric, pan-telomeric and CEN-specific centromeric, subtelomeric and painting DNA probes (reviewed by Zalensky, 1998; Zalenskaya and Zalensky, 2000). According to this model, territories of all chromosomes join in the internally located chromocenter, while the p-TEL and q-TEL domains of each chromosome interact at the nuclear periphery (Fig. 5A). Similar principles of the overall spatial chromosome organization in sperm are conserved in mammalian evolution, as indicated by data for other animals: cattle (Powell et al., 1990; Zalensky et al., 1997), mice (Haaf and Ward, 1995; Jennings and Powell, 1995; Meyer-Fica et al., 1998), boar, stallion, and rat (Zalensky et al., 1997). Therefore, nonrandom chromosome architecture in sperm, most probably have a functional significance.

Within the existing model (Fig. 5A), several important aspects remained unresolved, primarily the internal organization of CT in sperm, e.g. the path of the chromosome between CEN (chromocenter) and TEL, and ways of chromosome packaging above the level of nucleoprotamine toroids. Fig. 5B illustrates hierarchical archetypes of chromosome organization in human sperm established in this study.

In 'native' minimally decondensed cells (Fig. 5Ba), whose chromosomes are packed into the highly compact, slightly elongated territory, FISH signals originating from chromosome arms largely overlap and details of CT internal structure are hidden. These details were exposed by the nuclear swelling (Fig. 5Ba-d), which induces progressive unwinding of the compact CT. During the initial stage, CTs adopt shape of an elongated fibril with the average width of 2000±200 nm (Fig. 5Bb). Within this fibril, the domains of the p- and q- arm tightly interweave or lay parallel, p-TELs and q-TELs are joined, and chromosome threads bend at 180° near the CEN. In turn, chromatin of each arm is organized in 1000±120 nm filaments that often demonstrate spiral-type conformations (Fig. 5Bc). Filaments of 1000 nm are composed of the nodular structures with 500±70 nm in diameter, interconnected by thinner chromatin fibers (Fig. 5Bd). Apparently, two rows of the 500 nm chromatin beads merge into a 1000 nm thick fiber of a chromosome arm, as demonstrated in Fig. 4B. We speculate that each bead is composed of nucleoprotamine toroids (Balhorn et al., 1999), Fig. 5Be. To satisfy the observed bead size (500 nm) and knowing that dimensions of toroids are 25×60 to 100 nm, we conclude that each bead contains 100-200 toroids. This would correspond to 3-5 Mb of DNA, becasue each toroid packs to about 50 kb.

According to the donut-loop model of chromatin organization in mammalian sperm suggested by S. W. Ward (reviewed by Ward and Ward, 2004), nucleoprotamine toroids represent compacted DNA loops and are interconnected by nucleohistone DNA presumably attached to the sperm nuclear matrix (Fig. 5C). One of the experimental arguments in support of this model is the cleavage of sperm chromatin by nucleases, which liberates resistant fragments with the mean DNA size of 50 kb, a size that roughly corresponds to the length of DNA within toroid (Sotolongo et al., 2003). The model suggested in our work is relevant for the chromatin structures larger than 300 nm and thus neither supports nor disagrees with the donut-loop model by Ward.
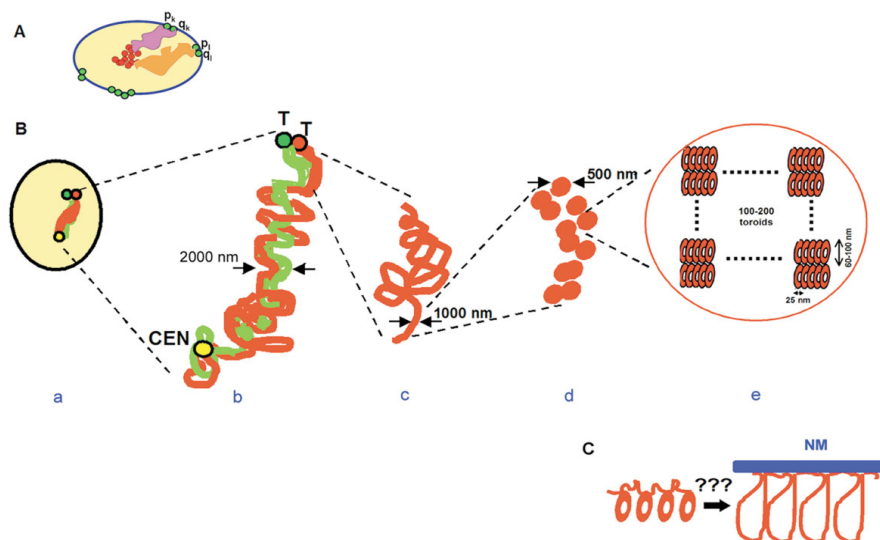

Fig. 5. Chromosome architecture in human sperm cells. (A) Model of sperm nuclear architecture proposed on the basis of CEN- and TEL-domain localization (Zalensky, 1988; Zalenskaya and Zalensky, 2000). Only two CTs (orange and pink areas) are shown. They stretch between the sperm chromocenter formed by an association of CENs (red circles) and TELs (green circles), which form dimers at the nuclear periphery. (B) Levels of chromosome architecture in human sperm nuclei, arm-specific chromatins are shown in red and green. (a) Compact CT, p- and q-arms are tightly merged. (b) Extended chromosome hairpin, arms are intertwined or stacked in antiparallel; (c) 1000 nm fiber of an individual arm; (d) Two rows of 500 nm nodular structures that form 1000 nm fiber. (e) Chromatin nodules hypothetically consist of nucleoprotamine toroids. CEN, centromere; T, telomere. (C) Donut-loop model (Ward and Ward, 2004). A thinner chromatin thread, presumably nucleohistone, attached to a nuclear matrix (NM) connects nucleoprotamine toroids. Each toroid consists of a packed 50 kb DNA loop.

Because of drastically different molecular characteristics of the basic structural proteins organizing DNA in the interphase nuclei (histones) and the sperm nuclei (protamines), all levels of chromatin/chromosome structures are different between these cell types. As a result, the hierarchy of structures established here for human sperm does not match that of nucleosomes or of chromatin fibers in interphase with diameters of 10 and 30 nm (Dehghani et al., 2005).

To what extent is the here proposed model of chromosome architecture for human spermatozoa applicable to sperm of other mammalian species? Although there are only few relevant experimental data, we propose the principles of chromosome organization are similar. The existence of CTs and their preferred nuclear positioning were demonstrated in sperms of boar (Foster et al., 2005), rodents (Haaf and Ward, 1995; Meyer-Ficca et al., 1998) and evolutionary distant non-eutherian mammals (Greaves et al., 2003; Grutzner et al., 2004). Probably, sperm chromosomes in other mammals are also in hairpin (looped) conformation because TEL dimers exists in mouse, rat, boar and bull (Zalensky et al., 1997; Meyer-Ficca et al., 1998). Finally, the internal structural elements of CTs, similar to those observed here for humans, are probably preserved in other mammals because sperm DNA is also packed with protamines.

Although the in-situ hybridization approach described here provides a reasonable view of sperm-chromosome organization – from 500 nm beads up to compact CTs – additional experiments combining biochemical and high-resolution microscopy techniques are needed to establish sperm chromatin organization on a 50-500 nm scale. We suggest that the described mode of chromosome packing in sperm is universal for all chromosomes; nonetheless, additional information on the architecture of the acrocentric and the short meta-centric chromosomes is desirable. We believe that information on the organization of sperm CT derived here from FISH experiments is significant, however, direct deduction of the chromosome architecture in vivo should be made with caution.

In conclusion, chromosomes in human sperm demonstrate elaborated spatial organization on all levels starting from the elementary units of DNA packing by protamines and up to the higher order structure of CTs. Furthermore, overall nuclear architecture in sperm is highly ordered as well: chromosomes demonstrate nonrandom intranuclear positions, are adhered with CENs in internal compact chromocenter and are exposed to nuclear periphery with specifically interacting TEL domains. Such unique nuclear architecture is most probably designed for the orchestrated unpacking and activation of the male genome during fertilization. Indeed, the timing and character for zygotic gene activation is determined by changes in chromatin structure, rather than changes in the activity of the transcriptional apparatus (Schultz and Worrad, 1995). Studies how the CT is unpacked during male pronuclei formation in systems modeling initial stages of human fertilization are in progress.

References

Allen, M. J., Bradbury, E. M. and Balhorn, R. (1997). AFM analysis of DNA-protamine complexes bound to mica. *Nucleic Acids Res.* **25**, 2221-2226.

Allison, D. C. and Nestor, A. L. (1999). Evidence for a relatively random array of human chromosomes on the mitotic ring. *J. Cell Biol.* **145**, 1-14.

Balhorn, R. (1982). A model for the structure of chromatin in mammalian sperm. *J. Cell Biol.* **93**, 298-305.

Balhorn, R., Cosman, M., Thornton, K., Krishnan, V. V., Corzett, M., Bench, G., Kramer, C., Lee, J., Hud, N. V., Allen, M. et al. (1999). Protamine-mediated condensation of DNA in mammalian sperm. In *The Male Gamete: from Basic Knowledge to Clinical Applications* (ed. C. Gagnon), pp. 55-70. Vienna, IL: Cache River Press.

Belmont, A. S., Dietzel, S., Nye, A. C., Strukov, Y. G. and Tumbar, T. (1999). Large-scale chromatin structure and function. *Curr. Opin. Cell Biol.* **11**, 307-311.

Boyle, S., Gilchrist, S., Bridger, J. M., Mahy, N. L., Ellis, J. A. and Bickmore, W. A. (2001). The spatial organization of human chromosomes within the nuclei of normal and emerin-mutant cells. *Hum. Mol. Genet.* **10**, 211-219.

Brandriff, B. F. and Gordon, L. A. (1992). Spatial distribution of sperm-derived chromatin in zygotes determined by fluorescence in situ hybridization. *Mutat. Res.* **296**, 33-42.

Brewer, L. R., Corzett, M. and Balhorn, R. (1999). Protamine-induced condensation and decondensation of the same DNA molecule. *Science* **286**, 120-123.

Brewer, L. R., Corzett, M., Lau, E. Y. and Balhorn, R. (2003). Dynamics of protamine 1 binding to single DNA molecules. *J. Biol. Chem.* **278**, 42403-42408.

Canapa, A., Cerioni, P. N., Barucca, M., Olmo, E. and Caputo, V. (2002). A centromeric satellite DNA may be involved in heterochromatin compactness in gobiid fishes. *Chromosome Res.* **10**, 297-304.

Cockell, M. and Gasser, S. M. (1999). Nuclear compartments and gene regulation. *Curr. Opin. Genet. Dev.* **9**, 199-205.

Cremer, T. and Cremer, C. (2001). Chromosome territories, nuclear architecture and gene regulation in mammalian cells. *Nat. Rev. Genet.* **2**, 292-301.

Cremer, M. K., Küpper, B., Wagler, L., Wizelmann, J., von Hase, Y., Weiland, L., Kreja, J., Diebold, M., Speicher, R. and Cremer, T. (2003). Inheritance of gene density-related higher order chromatin arrangements in normal and tumor cell nuclei. *J. Cell Biol.* **162**, 809-820.

Cremer, T., Kupper, K., Dietzel, S. and Fakan, S. (2004). Higher order chromatin architecture in the cell nucleus: on the way from structure to function. *Biol. Cell.* **96**, 555-567.

Dehghani, H., Dellaire, G. and Bazett-Jones, D. P. (2005). Organization of chromatin in the interphase mammalian cell. *Micron* **36**, 95-108.

Delgado, N. M., Huacuja, L., Merchant, H., Reyes, R. and Rosado, A. (1980). Species specific decondensation of human spermatozoa nuclei by heparin. *Arch. Androl.* **4**, 305-313.

Dietzel, S., Jauch, A., Kienle, D., Qu, G., Holtgreve-Grez, H., Eils, R., Munkel, C., Bittner, M., Meltzer, P. S., Trent, J. M. et al. (1998). Separate and variably shaped chromosome arm domains are disclosed by chromosome arm painting in human cell nuclei. *Chromosome Res.* **6**, 25-33.

Dietzel, S., Zolghadr, K., Hepperger, C. and Belmont, A. S. (2004). Differential large-scale chromatin compaction and intranuclear positioning of transcribed versus non-transcribed transgene arrays containing beta-globin regulatory sequences. *J. Cell Sci.* **117**, 4603-4614.

Dundr, M. and Misteli, T. (2001). Functional architecture in the cell nucleus. *Biochem. J.* **356**, 297-310.

Eissenberg, J. C. and Elgin, S. C. (2000). The HP1 protein family: getting a grip on chromatin. *Curr. Opin. Genet. Dev.* **10**, 204-210.

Fan, J. Y., Rangasamy, D., Luger, K. and Tremethick, D. J. (2004). H2A.Z alters the nucleosome surface to promote HP1alpha-mediated chromatin fiber folding. *Mol. Cell.* **16**, 655-661.

Fita, I., Campos, J. L., Puigjaner, L. C. and Subirana, J. A. (1983). X-ray diffraction study of DNA complexes with arginine peptides and their relation to nucleoprotamine structure. *J. Mol. Biol.* **167**, 157-177.

Foster, H. A., Abeydeera, L. R., Griffin, D. K. and Bridger, J. M. (2005). Non-random chromosome positioning in mammalian sperm nuclei, with migration of the sex chromosomes during late spermatogenesis. *J. Cell Sci.* **118**, 1811-1820.

Fraschini, A. and Biggiogera, M. (1985). Ultrastructural analysis of mouse sperm chromatin. *Basic Appl. Histochem.* **29**, 231-244.

Geraedts, J. P. and Pearson, P. L. 1975. Spatial distribution of chromosomes 1 and Y in human spermatozoa. *J. Reprod. Fertil.* **45**, 515-517.

Gerlich, D., Beaudouin, J., Kalbfuss, B., Daigle, N., Eils, R. and Ellenberg, J. (2003). Global chromosome positions are transmitted through mitosis in mammalian cells. *Cell.* **112**, 751-764.

Gineitis, A. A., Zalenskaya, I. A., Yau, P. M., Bradbury, E. M. and Zalensky, A. O. (2000). Human sperm telomere-binding complex involves

histone H2B and secures telomere membrane attachment. *J. Cell Biol.* **151**, 1591-1598.

Greaves, I. K., Rens, W., Ferguson-Smith, M. A., Griffin, D. and Marshall-Graves, J. A. (2003). Conservation of chromosome arrangement and position of the X in mammalian sperm suggests functional significance. *Chromosome Res.* **11**, 503-512.

Grutzner, F., Rens, W., Tsend-Ayush, E., El-Mogharbel, N., O'Brien, P. C., Jones, R. C., Ferguson-Smith, M. A. and Marshall Graves, J. A. (2004). In the platypus a meiotic chain of ten sex chromosomes shares genes with the bird Z and mammal X chromosomes. *Nature* **432**, 913-917.

Gusse, M. and Chevaillier, P. (1980). Electron microscope evidence for the presence of globular structures in different sperm chromatins. *J. Cell Biol.* **87**, 280-284.

Haaf, T. and Ward, D. C. (1995). Higher order nuclear structure in mammalian sperm revealed by in situ hybridization and extended chromatin fibers. *Exp. Cell Res.* **219**, 604-611.

Hazzouri, M., Rousseaux, S., Mongelard, F., Usson, Y., Pelletier, R., Faure, A. K., Vourc'h, C. and Sele, B. (2000). Genome organization in the human sperm nucleus studied by FISH and confocal microscopy. *Mol. Reprod. Dev.* **55**, 307-315.

Hoyer-Fender, S., Singh, P. B. and Motzkus, D. (2000). The murine heterochromatin protein M31 is associated with the chromocenter in round spermatids and is a component of mature spermatozoa. *Exp. Cell Res.* **254**, 72-79.

Hud, N. V., Allen, M. J., Downing, K. H., Lee, J. and Balhorn, R. (1993). Identification of the elemental packing unit of DNA in mammalian sperm cells by atomic force microscopy. *Biochem. Biophys. Res. Commun.* **193**, 1347-1354.

Jennings, C. and Powell, D. (1995). Genome organization in the murine sperm nucleus. *Zygote* **3**, 123-131.

Kreth, G., Finsterle, J., von Hase, J., Cremer, M. and Cremer, C. (2004). Radial arrangement of chromosome territories in human cell nuclei: a computer model approach based on gene density indicates a probabilistic global positioning code. *Biophys. J.* **86**, 2803-2812.

Leitch, A. R., Brown, J. K., Mosgoller, W., Schwarzacher, T. and Heslop-Harrison, J. S. (1994). The spatial localization of homologous chromosomes in human fibroblasts at mitosis. *Hum. Genet.* **93**, 275-280.

Lowenstein, M. G., Goddard, T. D. and Sedat, J. W. (2004). Long-range interphase chromosome organization in Drosophila: a study using color barcoded fluorescence in situ hybridization and structural clustering analysis. *Mol. Biol. Cell* **15**, 5678-5692.

Luetjens, C. M., Payne, C. and Schatten, G. (1999). Non-random chromosome positioning in human sperm and sex chromosome anomalies following intracytoplasmic sperm injection. *Lancet* **353**, 1240.

Luzatti, V. and Nicolaeff, A. C. R. (1959). Central diffusion x-ray study on the structure of nucleoprotamine and nucleohistone aqueous gels and of intact nuclei. *C. R. Hebd. Seances Acad. Sci.* **248**, 1426-1429.

Martianov, I., Brancorsini, S., Gansmuller, A., Parvinen, M., Davidson, I. and Sassone-Corsi, P. (2002). Distinct functions of TBP and TLF/TRF2 during spermatogenesis: requirement of TLF for heterochromatic chromocenter formation in haploid round spermatids. *Development* **129**, 945-955.

McLay, D. W. and Clarke, H. J. (2003). Remodeling the paternal chromatin at fertilization in mammals. *Reproduction* **125**, 625-633.

Meyer-Ficca, M., Muller-Navia, J. and Scherthan, H. (1998). Clustering of pericentromeres initiates in step 9 of spermiogenesis of the rat (Rattus norvegicus) and contributes to a well defined genome architecture in the sperm nucleus. *J. Cell Sci.* **111**, 1363-1370.

Nagele, R., Freeman, T., McMorrow, L. and Lee, H. Y. (1995). Precise spatial positioning of chromosomes during prometaphase: evidence for chromosomal order. *Science* **270**, 1831-1835.

Parada, L. A., McQueen, P. G. and Misteli, T. (2004). Tissue-specific spatial organization of genomes. *Genome Biol.* **5**, R44.

Perrini, B., Piacentini, L., Fanti, L., Altieri, F., Chichiarelli, S., Berloco, M., Turano, C., Ferraro, A. and Pimpinelli, S. (2004). HP1 controls telomere capping, telomere longation, and telomere silencing by two different mechanisms in Drosophila. *Mol. Cell.* **15**, 467-476.

Powell, D., Cran, D. G., Jennings, C. and Jones, R. (1990). Spatial organization of repetitive DNA sequences in the bovine sperm nucleus. *J. Cell Sci.* **97**, 185-191.

Romanato, M., Cameo, M. S., Bertolesi, G., Baldini, C., Calvo, J. C. and Calvo, L. (2003). Heparan sulphate: a putative decondensing agent for human spermatozoa in vivo. *Hum. Reprod.* **18**, 1868-1873.

Sanchez-Vazquez, M. L., Reyes, R., Ramirez, G., Merchant-Larios, H., Rosado, A. and Delgado, N. M. (1998). DNA unpacking in guinea pig sperm chromatin by heparin and reduced glutathione. *Arch. Androl.* **40**, 15-28.

Schardin, M., Cremer, T., Hager, H. D. and Lang, M. (1985). Specific staining of human chromosomes in Chinese hamster × man hybrid cell lines demonstrates interphase chromosome territories. *Hum. Genet.* **71**, 281-287.

Schultz, R. M. and Worrad, D. M. (1995). Role of chromatin structure in zygotic gene activation in the mammalian embryo. *Semin. Cell Biol.* **6**, 201-208.

Sobhon, P., Chutatape, C., Chalermisarachai, P., Vongpayabal, P. and Tanphaichitr, N. (1982). Transmission and scanning electron microscopic studies of the human sperm chromatin decondensed by micrococcal nuclease and salt. *J. Exp. Zool.* **221**, 61-79.

Solov'eva, L., Svetlova, M., Bodinski, D. and Zalensky, A. O. (2004). Nature of telomere dimers and chromosome looping in human spermatozoa. *Chromosome Res.* **12**, 817-823.

Sotolongo, B., Lino, E. and Ward, W. S. (2003). Ability of hamster spermatozoa to digest their own DNA. *Biol. Reprod.* **69**, 2029-2035.

Stack, S. M., Brown, D. B. and Dewey, W. C. (1977). Visualization of interphase chromosomes. *J. Cell Sci.* **26**, 281-299.

Stadler, S., Schnapp, V., Mayer, R., Stein, S., Cremer, C., Bonifer, C., Cremer, T. and Dietzel, S. (2004). The architecture of chicken chromosome territories changes during differentiation. *BMC Cell Biol.* **5**, 44.

Sutovsky, P. and Schatten, G. (1997). Depletion of glutathione during bovine oocyte maturation reversibly blocks the decondensation of the male pronucleus and pronuclear apposition during fertilization. *Biol. Reprod.* **56**, 1503-1512.

Taddei, A., Hediger, F., Neumann, F. R. and Gasser, S. M. (2004). The function of nuclear architecture: a genetic approach. *Ann. Rev. Genet.* **38**, 305-345.

Terada, Y., Luetjens, C. M., Sutovsky, P. and Schatten, G. (2000). Atypical decondensation of the sperm nucleus, delayed replication of the male genome, and sex chromosome positioning following intracytoplasmic human sperm injection (ICSI) into golden hamster eggs: does ICSI itself introduce chromosomal anomalies? *Fertil. Steril.* **74**, 454-460.

Tilgen, N., Guttenbach, M. and Schmid, M. (2001). Heterochromatin is not an adequate explanation for close proximity of interphase chromosomes 1–Y, 9–Y, and 16–Y in human spermatozoa. *Exp. Cell Res.* **265**, 283-287.

van Driel, R., Fransz, P. F. and Verschure, P. J. (2003). The eukaryotic genome: a system regulated at different hierarchical levels. *J. Cell Sci.* **116**, 4067-4075.

Villeponteau, B. (1992). Heparin increases chromatin accessibility by binding the trypsin-sensitive basic residues in histones. *Biochem. J.* **288**, 953-958.

Walter, J., Schermelleh, L., Cremer, M., Tashiro, S. and Cremer, T. (2003). Chromosome order in HeLa cells changes during mitosis and early G1, but is stably maintained during subsequent interphase stages. *J. Cell Biol.* **160**, 685-697.

Ward, M. A. and Ward, W. S. (2004). A model for the function of sperm DNA degradation. *Reprod. Fertil. Dev.* **16**, 547-554.

Ward, W. S. and Coffey, D. S. (1991). DNA packaging and organization in mammalian spermatozoa: comparison with somatic cells. *Biol. Reprod.* **44**, 569-574.

Yaron, Y., Kramer, J. A., Gyi, K., Ebrahim, S. A., Evans, M. I., Johnson, M. P. and Krawetz, S. A. (1998). Centromere sequences localize to the nuclear halo of human spermatozoa. *Int. J. Androl.* **21**, 13-18.

Zalenskaya, I. A. and Zalensky, A. O. (2000). Telomeres in mammalian germ-line cells. *Intern. Rev. Cytology.* **218**, 37-67.

Zalenskaya, I. A. and Zalensky, A. O. (2004). Non-random positioning of chromosomes in human sperm nuclei. *Chromosome Res.* **12**, 163-173.

Zalensky, A. O. (1998). Genome Architecture. *In Advances in Genome Biology* (ed. R. S. Verma), pp. 179-210. Greenwich, London: JAI Press.

Zalensky, A. O., Breneman, J. W., Zalenskaya, I. A., Brinkley, B. R. and Bradbury, E. M. (1993). Organization of centromeres in the decondensed nuclei of mature human sperm. *Chromosoma* **102**, 509-518.

Zalensky, A. O., Allen, M. J., Kobayashi, A., Zalenskaya, I. A., Balhorn, R. and Bradbury, E. M. (1995). Well-defined genome architecture in the human sperm nucleus. *Chromosoma* **103**, 577-590.

Zalensky, A. O., Tomilin, N. V., Zalenskaya, I. A., Teplitz, R. L. and Bradbury, E. M. (1997). Telomere-telomere interactions and candidate telomere binding protein(s) in mammalian sperm cells. *Exp. Cell Res.* **232**, 29-41.